minerals

MDPI

Article

Experimental Study on the Thickening Characteristics of Ultrafine Tailings

Jiandong Wang [1,2,3], Zhaolong Du [1,2,3], Xiaohui Liu [4,*] and Aixiang Wu [1,2,3]

[1] School of Resources and Safety Engineering, University of Science and Technology Beijing, Beijing 100083, China; wangjiandong@ustb.edu.cn (J.W.); du1981171802@163.com (Z.D.); wuaixiang@126.com (A.W.)
[2] Key Laboratory of Safe and Green Mining of Metal Mines with Cemented Paste Backfill, National Mine Safety Administration, University of Science and Technology Beijing, Beijing 100083, China
[3] Key Laboratory of Ministry of Education for Efficient Mining and Safety of Metal Mines, University of Science and Technology Beijing, Beijing 100083, China
[4] School of Safety Engineering, North China Institute of Science and Technology, Hebei 065201, China
* Correspondence: liuxiaohui28@ncist.edu.cn

Abstract: To investigate the thickening characteristics of ultrafine tailings and the relationship between bed height and underflow concentration, a series of experiments, including graduated cylinder sedimentation tests, small-scale dynamic thickening, and semi-industrial experiments, were conducted. The results show that adding flocculants accelerates settling velocity, with a significant change occurring at 50 g/t when the bridging effect weakens. Solid flux increases initially with feed concentration but decreases after reaching a peak at 8%, where the maximum solid flux is 0.322 $t \cdot m^{-2} \cdot h^{-1}$. Reducing solid flux, lowering flocculant dosage, and increasing bed height all contribute to higher underflow concentration, while reducing solid flux and increasing flocculant dosage lowers overflow turbidity. The variation in underflow concentration in the deep cone thickener (DCT) occurs in three phases: continuous feeding with no discharge, dynamic equilibrium with a stable bed height, and bed descent with increasing underflow discharge. At the same bed height, underflow concentration is lower during the bed descent phase compared to the continuous feeding phase. This study offers valuable insights for the precise control of underflow concentration in ultrafine tailing thickening processes.

Keywords: ultrafine tailings; thickening; flocculant; underflow concentration; bed height

check for updates

Academic Editor: Abbas Taheri

Received: 30 November 2024
Revised: 15 January 2025
Accepted: 20 January 2025
Published: 22 January 2025

Citation: Wang, J.; Du, Z.; Liu, X.; Wu, A. Experimental Study on the Thickening Characteristics of Ultrafine Tailings. *Minerals* **2025**, *15*, 100. https://doi.org/10.3390/min15020100

Copyright: © 2025 by the authors. Licensee MDPI, Basel, Switzerland. This article is an open access article distributed under the terms and conditions of the Creative Commons Attribution (CC BY) license (https://creativecommons.org/licenses/by/4.0/).

1. Introduction

The rapid advancement of human society heavily depends on mineral resources. However, mining activities produce vast amounts of tailings, the surface storage of which leads to numerous challenges. These include the consumption of land resources, environmental degradation, and safety hazards [1,2]. In recent years, cemented paste backfill (CPB) has emerged as a widely adopted solution for managing the substantial quantities of tailings generated by metal mining operations, owing to its advantages in safety, environmental sustainability, efficiency, and cost-effectiveness [3–5]. This technique involves thickening the low-concentration tailing slurry discharged from the processing plant and then mixing it with water, binder, and other additives to form a highly concentrated, flowable paste. The prepared paste is subsequently transported to underground voids by gravity or pump [6]. The initial and critical step in CPB technology is the thickening of the tailing slurry. This process utilizes polymer flocculants and the synergistic effects of shear stress from the

deep cone thickener's rake and the slurry's own gravitational stress to concentrate the low-density feed into a high-concentration underflow [7,8].

Currently, tailings produced by mineral processing plants are typically very fine, possessing a small particle size. It is often not possible to utilize all of the tailings, making it necessary to adopt classification techniques. In this approach, coarse tailings from classification processes are often repurposed as construction materials [9,10], while ultrafine tailings are used for underground backfilling. Therefore, the flocculation and thickening process for ultrafine tailings has become a critical focus of research, with extensive studies exploring factors such as flocculation performance [11,12] and floc structure [13,14].

Innovative flocculants and advanced methods have significantly improved the flocculation and dewatering performance of ultrafine tailings. For instance, tannic acid-mediated polymer networks have enhanced the dewatering of mature oil sand tailings, producing stronger flocs and improving filter cake permeability [15]. Response surface methodology has highlighted the synergistic effects of Na^+ and Ca^{2+} concentrations with anionic polyacrylamide dosage, while dual flocculation processes have proven highly effective in capturing fine particles and forming larger flocs [16,17]. Additionally, alkoxy silane has been used to achieve underflow concentrations exceeding 42 wt% and reduced overflow turbidity, facilitating water reuse [18].

Further research on ultrafine tailings has linked flocculation to increased yield stress with higher pH and flocculant dosage, leading to a yield stress model based on flocculant adsorption [19]. Moreover, studies based on superflocculation theory have identified optimal conditions for parameters such as pH, flocculant dosage, and shear rate [20]. In addition to experimental methods, computational methods have expanded the understanding of flocculation dynamics. A population balance model has been applied to describe the aggregation and breakage of flocs in saltwater [21]. Hybrid machine learning methods, such as combining particle swarm optimization (PSO) with adaptive neuro-fuzzy inference systems (ANFISs), have enhanced the predictive accuracy of flocculation and dewatering performance [22].

This study systematically explores the thickening characteristics of ultrafine tailings through a series of experiments. Graduated cylinder sedimentation tests were firstly conducted to determine the optimal thickening parameters. Small-scale dynamic thickening experiments were then performed to examine the effects of varying solid fluxes and specific flocculant dosages on the underflow concentration and overflow turbidity of the slurry, validating the rationality of the optimal parameters. Finally, semi-industrial deep cone thickening experiments were conducted to simulate high mud layer pressure, exploring the intrinsic relationship between mud bed height and underflow concentration under various operating conditions. This research provides theoretical guidance and practical insights for optimizing thickening processes in tailing management and advancing the efficient utilization of resources.

2. Materials and Methods

2.1. Materials

The raw materials used in this study include classified ultrafine tailings, flocculants, and water. The ultrafine tailings were derived from a lead-zinc mine in Guangdong Province, China, by classifying the full tailings generated at the mine's processing plant. The classification was performed using a hydrocyclone, where the tailing slurry was fed under controlled pressure and flow conditions. This process separated the particles based on their size and density, with the fine fraction collected from the overflow and the coarser fraction discharged through the underflow. Four nonionic polyacrylamide flocculants were selected: FA4000 (molecular weight 8×10^6), N1134S (9.5×10^6), AS02 (1×10^7), and

781-8-25 (1.6×10^7). Tap water was used to prepare both the slurry and the flocculant solution during the experiments.

The solid densities of the full tailings and classified ultrafine tailings measured using the water pycnometer test were 3.104 g/cm^3 and 3.063 g/cm^3. The particle size distribution of both types of tailings was analyzed using a TopSizer Laser Particle Size Analyzer (OMEC Instruments Co., Ltd., Zhuhai, China), as shown in Figure 1. The characteristic particle diameter D_x, representing the particle size with x vt.% of tailings smaller than this size, can be obtained from Figure 1, where D_{10}, D_{50}, and D_{90} for the classified ultrafine tailings are 1.71 μm, 9.43 μm, and 42.45 μm, respectively, and for the full tailings they are 3.02 μm, 15.83 μm, and 64.75 μm, respectively.

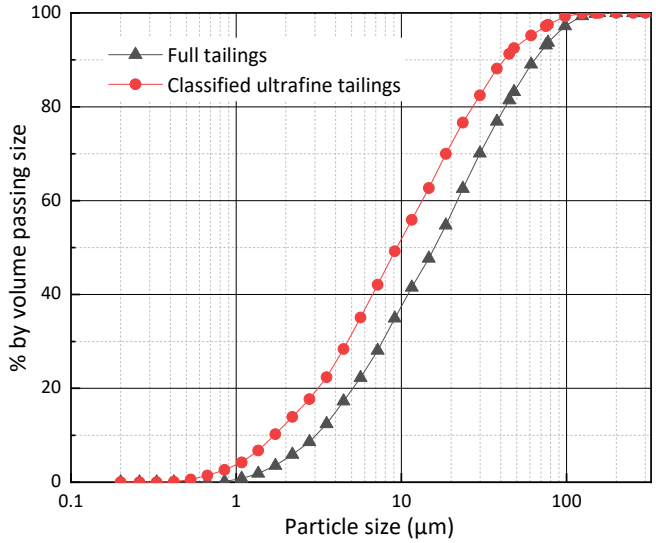

Figure 1. Particle size distribution of full tailings and classified ultrafine tailings.

2.2. Experimental Equipment

The experimental equipment used in this study included 500 mL graduated cylinders with grid lines, beakers, a stirrer, a small-scale dynamic thickening device, and a semi-industrial deep cone thickener (DCT). The small-scale dynamic thickening device, shown in Figure 2, features a transparent settling column with a height of 1 m and a radius of 0.18 m. Two peristaltic pumps deliver the tailing slurry and flocculant solution into the settling column at controlled rates. A rake structure inside the settling column applies shear motion to the tailing slurry, and the thickened slurry is discharged through an outlet at the bottom.

As shown in Figure 3, the semi-industrial DCT consists of a small DCT, a flocculant solution preparation and dosing system, a slurry feeding system, an underflow discharge system, and an overflow discharge system. The small DCT features an inner diameter of 1 m, a cone height of 1 m, and a cylindrical section height of 9 m. It can simulate the dynamic thickening process under high mud layer pressure in industrial DCTs.

2.3. Experimental Scheme Design

2.3.1. Graduated Cylinder Sedimentation Test

The tailing samples were collected in multiple batches and then prepared using the quartering method, dried, and crushed. The tailing slurry was prepared in a graduated cylinder with grid lines, to which a flocculant solution was added. The cylinder was inverted three times to ensure thorough mixing, and then placed flat on a table. The sedimentation height was observed and recorded at various time intervals [23].



Figure 2. Small-scale dynamic thickening device.



Figure 3. Semi-industrial deep cone thickener.

The control variable method was used to investigate the effects of flocculant type, optimal tailing slurry concentration, and flocculant consumption on the sedimentation performance of tailings. The sedimentation height was monitored over time. First, the optimal flocculant type was determined. In this experiment, the tailing slurry concentration was set to 15 wt%, the flocculant consumption to 30 g/t, and the flocculant solution concentration to 0.02%. Next, based on the chosen optimal flocculant, sedimentation experiments were conducted at different tailing slurry concentrations (4 wt%, 8 wt%, 12 wt%, and 16 wt%), with solid flux as the indicator to determine the optimal feeding concentration. Finally, using the best flocculant and optimal slurry concentration, sedimentation experiments were performed under various flocculant consumption rates (10, 30, 50, 70, and 90 g/t). The average sedimentation rate over the first 3 min under each consumption condition was used to determine the optimal flocculant consumption rate.

2.3.2. Small-Scale Dynamic Thickening Experiment

Based on the results of the graduated cylinder sedimentation test, a two-factor, four-level dynamic thickening experiment was conducted using a transparent settling column to investigate the effects of different solid fluxes and flocculant dosages on key thickening parameters. The solid flux levels were set to 0.2, 0.3, 0.4, and 0.5 $t \cdot m^{-2} \cdot h^{-1}$, while the flocculant dosages were 40, 50, 60, and 70 g/t. To prevent excessive rake resistance, the rake rotation speed was set to 3 r/min, and the mud bed height was designed to reach 65 cm. Once the mud bed reached this height, underflow recirculation began. After 2–4 h of recirculation, the underflow concentration and overflow turbidity of the slurry were measured to evaluate the thickening performance [24,25].

2.3.3. Semi-Industrial Thickening Experiment

Based on the optimal parameters determined from previous experiments, including flocculant type, tailing slurry concentration, solid flux, and flocculant dosage, a semi-industrial thickening experiment was conducted. The experiment was controlled using a PLC system, which regulates the rake rotation speed, feed flow rate, and discharge flow rate.

Initially, the feed pump was activated, and the bed height gradually increased, entering the continuous feeding phase with no discharge. Once the bed height reached 8 m, the underflow pump was turned on to stabilize the bed height, marking the transition into the dynamic equilibrium phase. As the underflow discharge was gradually increased, the bed height began to decrease, entering the bed descent phase. The experiment investigated the variation in underflow concentration in DCT with respect to bed height during the continuous feeding, dynamic equilibrium, and bed descent phases. The study also explored the internal relationships between these phases, providing insights into the dynamic behavior of the thickening process.

3. Results and Discussion

3.1. Graduated Cylinder Sedimentation Test

Four nonionic flocculants were selected for sedimentation experiments, with a control group that contained no flocculant. The sedimentation height variation curve of the slurry is shown in Figure 4. The initial height was 240 mm, and after 30 min of sedimentation, the final height of the mud layer was approximately 80 mm. Comparing the sedimentation height changes during the first 10 min across all groups, it was found that the larger the molecular weight of the flocculant, the faster the sedimentation rate. However, when the molecular weight reached 10,000,000, its effect on the sedimentation rate became negligible.

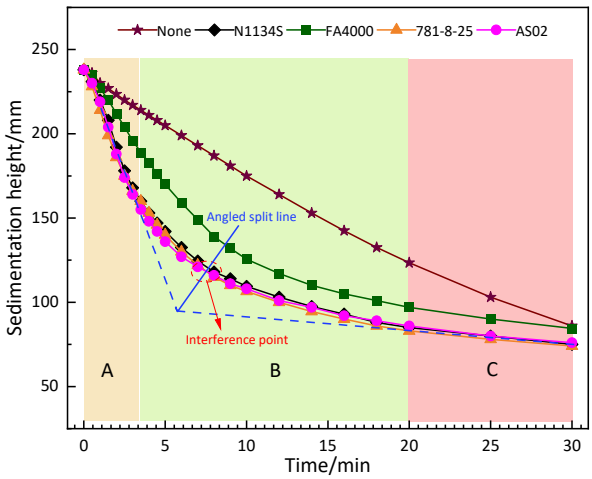

Figure 4. Sedimentation height variation curve of ultrafine tailing slurry.

The sedimentation curves of the flocculant groups can be divided into three stages. Stage A is the free settling region, where the sedimentation curve approximates a straight line with a constant settling velocity. Stage B is the interference settling region, where the sedimentation curve is concave and the settling velocity decreases over time. Stage C is the compression region, where the sedimentation curve levels off and the settling velocity stabilizes.

A linear analysis of the sedimentation curve for the no-flocculant group yielded a slope of −5.291 mm/min, with a high goodness-of-fit (R^2 = 0.99), indicating that the no-flocculant group remained in the free settling stage throughout the experiment. By comparing the slopes of the sedimentation curves in Stage A, it was found that the flocculant 781-8-25 exhibited the fastest settling velocity and the best sedimentation effect, making it the optimal choice for subsequent experiments.

Taking the sedimentation curve of the slurry corresponding to the 781-8-25 flocculant in Figure 4 as an example, the intersection point of the extended lines of the free settling region and the compression region is considered as the vertex. A bisector is drawn from this vertex to the sedimentation curve, and the point where the bisector intersects the curve is identified as the interference point. The settling velocity at the interference point is then substituted into Equation (1) to obtain the solid flux. As shown in Figure 5, with an increase in the feed solid mass fraction, both the settling velocity and solid flux initially increase and then decrease. When the feed solid mass fraction reaches 8%, the solid flux reaches its relative maximum value of 0.322 $t \cdot m^{-2} \cdot h^{-1}$.

$$G_S = \rho_S C_V v \times 60 \times 10^{-6} \quad (1)$$

where G_S is the solid flux ($t \cdot m^{-2} \cdot h^{-1}$), ρ_S is the tailing density ($kg \cdot m^{-3}$), C_V is the solid volume fraction at the interference point (%), and v is the settling velocity at the interference point (mm/min).

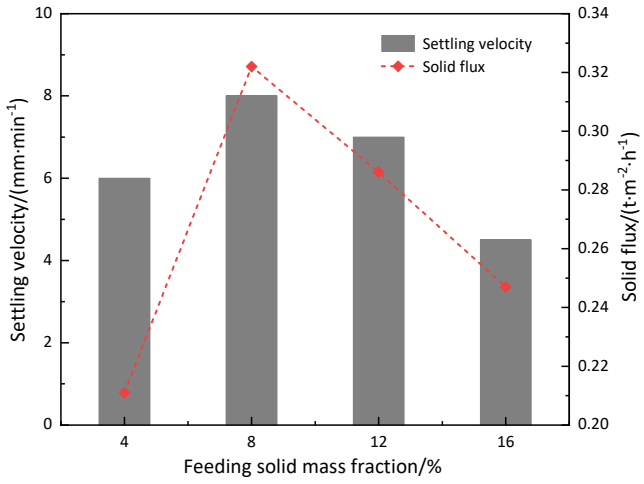

Figure 5. Sedimentation characteristics of slurry at different solid concentrations.

The sedimentation characteristic curve of the slurry under different flocculant dosages is shown in Figure 6. The settling velocity increases with the flocculant dosage. However, when the dosage reaches around 50 g/t, a noticeable change in the curve occurs, with the rate of increase in settling velocity decreasing from 1.1 to 0.27. This indicates that at lower flocculant dosages, the flocculant effectively bridges and adsorbs between tailing particles, connecting free particles to form a network structure. When the dosage becomes too high, the limited surface sites on the tailing particles are occupied by excessive high-molecular-weight flocculant, preventing further bridging between particles. As a result, the bridging effect weakens, leading to the formation of stable ionic structures with no

available bridging sites. The steric hindrance effect of the polymer adsorption film also causes the particles to return to a stable, dispersed state, reducing the rate of increase in settling velocity. Additionally, an excessive flocculant dosage increases the yield stress of the slurry, negatively affecting its flowability [26,27]. Therefore, the optimal flocculant dosage is determined to be 50 g/t.

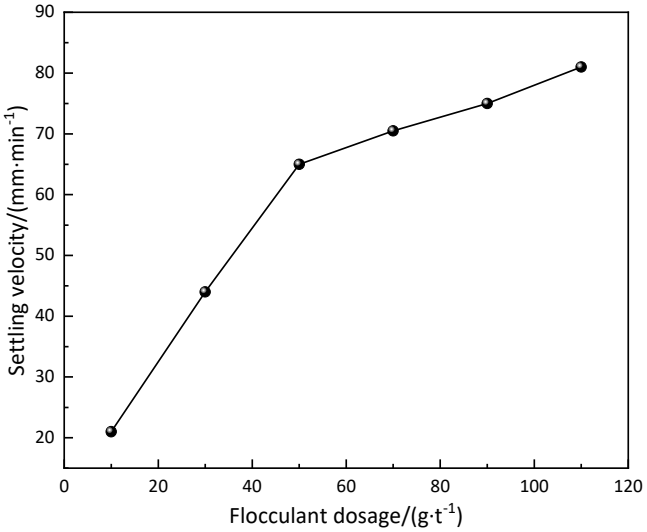

Figure 6. Sedimentation characteristics of slurry at different flocculant dosages.

3.2. Small-Scale Dynamic Thickening Experiment

During the small-scale dynamic thickening experiment, due to the limited bed height and poor compressive dewatering effect, the variations in overflow turbidity and underflow concentration over time were not significant. Therefore, the average values of the experimental data were used as the final results. The dynamic thickening characteristics of ultrafine tailings are shown in Figure 7. As the solid flux increases and the flocculant dosage decreases, the concentration of suspended particles in the overflow increases, leading to higher turbidity. In contrast, when the solid flux and flocculant dosage are relatively lower, the underflow concentration increases. A regression analysis of these changes was performed, as shown in Equations (2) and (3). The regression models for overflow turbidity and underflow concentration of thickened ultrafine tailings both follow a polynomial 2D function, with correlation coefficients (R^2) of 0.99, indicating high reliability.

$$y_1 = 104.11 + 869.81x_1 - 5.49x_2 - 8.375x_1^2 + 0.062x_2^2 - 10.079x_1x_2 \quad (2)$$

$$y_2 = 56.593 + 0.372x_1 + 0.01x_2 - 1.81x_1^2 - 1.94 \times 10^{-4}x_2^2 - 0.0013x_1x_2 \quad (3)$$

where x_1 is the solid flux ($t \cdot m^{-2} \cdot h^{-1}$), x_2 is the flocculant dosage (g/t), y_1 is the overflow turbidity (ppm), and x_2 is the underflow concentration (%).

From Equations (2) and (3), it can be seen that the solid flux is negatively correlated with underflow concentration and positively correlated with overflow turbidity. This is because slurry with a lower solid flux requires more time to reach the same bed height. Additionally, the flocculated network structure is compressible, and under the sustained pressure from the upper mud bed, it can expel more free water from the network structures. A higher solid flux also enhances slurry disturbance, leading to an increase in the number of suspended particles [28]. Therefore, although a higher solid flux improves tailing thickening efficiency, it also increases the risk of low underflow concentration and high overflow turbidity. Based on practical considerations, a solid flux of 0.25 $t \cdot m^{-2} \cdot h^{-1}$ is determined to be optimal.

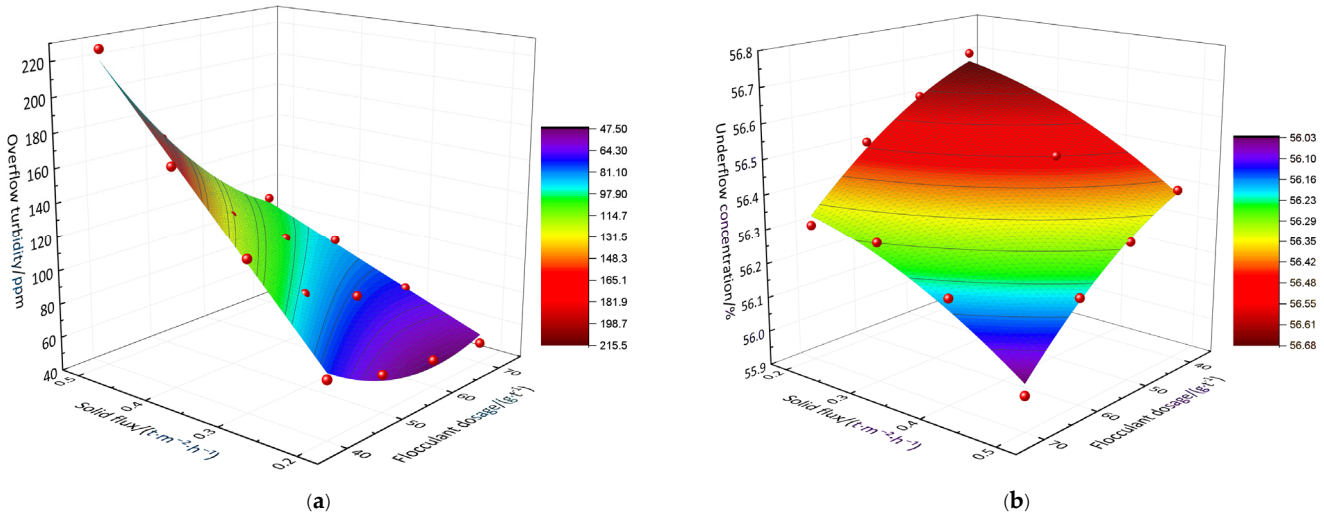

(**a**) (**b**)

Figure 7. Dynamic thickening characteristics of ultrafine tailings: (**a**) overflow turbidity and (**b**) underflow concentration.

The flocculant dosage is negatively correlated with both the underflow concentration and overflow turbidity. This is because the flocculant facilitates the aggregation of free tailing particles into flocs. Increasing the flocculant dosage enhances the flocculation of suspended particles, which further reduces the concentration of suspended solids. However, an excessive flocculant dosage can cause the tailing particles to become encapsulated in independent flocs, trapping large amounts of water within and between the flocs. This trapped water becomes difficult to expel, resulting in a decrease in underflow concentration [29]. Therefore, the flocculant dosage should be kept as low as possible, while ensuring that the overflow turbidity does not exceed the required threshold.

The mine requires that the overflow turbidity remains below 100 ppm. By substituting a solid flux of 0.25 $t \cdot m^{-2} \cdot h^{-1}$ and a flocculant dosage of 40 g/t into Equation (2), the resulting overflow turbidity is 99.84 ppm, which is very close to the threshold. For safety, the optimal flocculant dosage is therefore set to 50 g/t, which also aligns with the results from previous graduated cylinder sedimentation tests. A verification experiment was carried out using a solid flux of 0.25 $t \cdot m^{-2} \cdot h^{-1}$ and a flocculant dosage of 50 g/t. The measured overflow turbidity was 77.06 ppm, and the underflow concentration was 59.5%. Substituting these values into Equations (2) and (3) yielded predicted values for the overflow turbidity and underflow concentration of 75.55 ppm and 56.57%, respectively, with deviations of 1.96% and 4.92%. These results confirm the reliability of the fitting models.

3.3. Semi-Industrial Thickening Experiment

Under the optimal thickening parameters, the time-dependent variations in the bed height and underflow concentration of DCT during the semi-industrial experiment are shown in Figure 8. The first 30 h represent the continuous feeding phase with no discharge. When the bed height reaches 3 m, the underflow concentration is 50.5%; at 6.1 m, it increases to 56.9%; and at 8 m, it reaches 59.2%. The underflow concentration rises with the increase in bed height, which can be attributed to the higher pressure at the bottom of the thickener as the bed height increases, resulting in more significant slurry compression.

From 30 to 35 h, the system enters the dynamic equilibrium phase, during which the bed height stabilizes at 8 m. In the first 3 h of this phase, the underflow concentration decreases from 59.2% to 58.6%, and then remains stable at 58.6% for the next 2 h. This change occurs because high-concentration slurry is discharged from the bottom, while low-concentration

slurry from the upper layers moves downward to replenish the underflow. As the feeding and discharging rates reach equilibrium, the underflow concentration stabilizes.

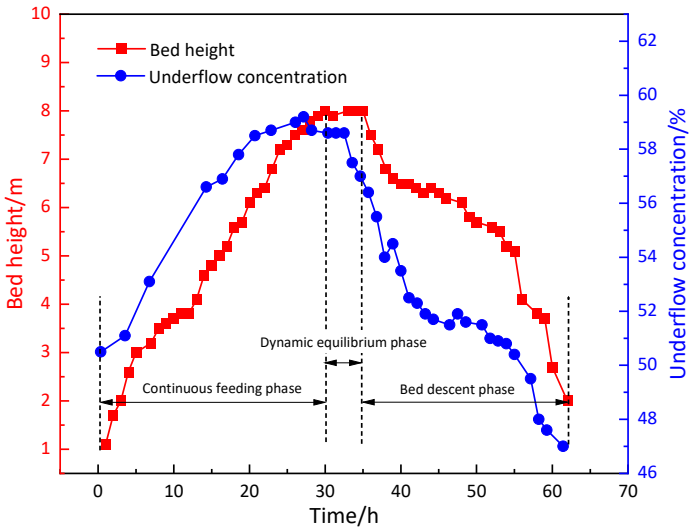

Figure 8. Time-varying curves of bed height and underflow concentration of DCT during the semi-industrial experiment.

From 35 to 63 h, the system enters the bed descent phase, during which the underflow concentration continues to decrease. When the bed height drops to 2 m, the underflow concentration falls to 47.5%. This decrease is caused by the reduction in bed height, which weakens the bed pressure and diminishes the thickening and dewatering efficiency of the slurry.

As shown in Figure 9, the relationship between underflow concentration and bed height during the continuous feeding and bed descent phases is fitted to obtain the predictive model for underflow concentration corresponding to bed height. During the continuous feeding phase, the underflow concentration initially increases slowly (1–4 m), then rises rapidly (4–7 m), and finally stabilizes (7–8 m). The regression equation for this phase is denoted as y_{phase1}, with a correlation coefficient (R^2) of 0.99. During the bed descent phase, the underflow concentration first decreases slowly (7–8 m) and then drops rapidly (2–7 m). When the bed height decreases from 4 m to 2 m, the underflow concentration decreases sharply. This is due to the insufficient bed height, where tailing particles primarily settle through free settling and interference settling. In this region, particles settle under their own weight and are unable to undergo effective compaction. The regression equation for this phase is denoted as y_{phase3}, with a correlation coefficient (R^2) of 0.96.

A comparison reveals that, at the same bed height, the underflow concentration during the bed descent phase is lower than during the continuous feeding phase with no discharge. This is because, during the bed descent phase, the tailings spend less time in DCT and are discharged as underflow before they have been subjected to sufficient bed pressure for effective compression.

The main factors influencing the underflow concentration of DCT are the shear action of the rake and the gravitational compaction of the bed. Since the shear action of the rake was fully utilized during the experiment, the primary cause of the differences in underflow concentration can be attributed to the gravitational compaction of the bed under different bed height conditions. Therefore, the underflow concentration can be controlled by adjusting the bed height, thereby producing slurry that meets the requirements for paste preparation.

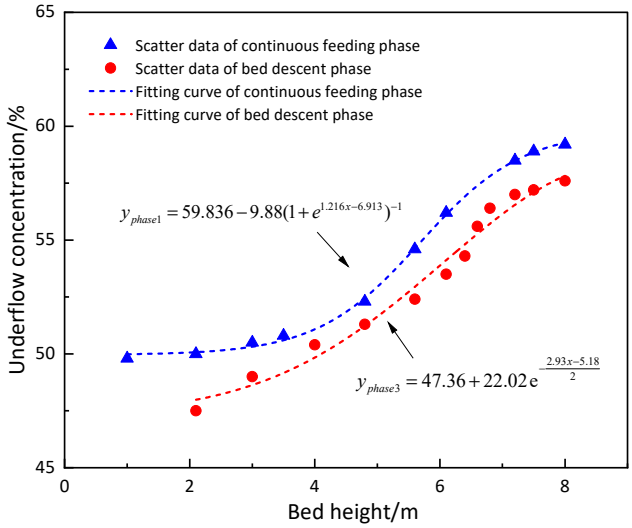

Figure 9. Relationship between bed height and underflow concentration of DCT during the semi-industrial experiment.

4. Conclusions

This study investigated the thickening characteristics of ultrafine tailings from a lead-zinc mine. Through graduated cylinder sedimentation tests, small-scale dynamic thickening experiments, and semi-industrial experiments, the effects of various process parameters on the thickening performance of DCT were examined, leading to the following key conclusions:

(1) The best sedimentation effect can be achieved using the nonionic flocculant 781-8-25. The optimal parameters are a feed concentration of 8%, a flocculant dosage of 50 g/t, and a solid flux of 0.25 $t \cdot m^{-2} \cdot h^{-1}$. In small-scale dynamic thickening experiments with these conditions, the overflow turbidity was 77.06 ppm, and the underflow concentration was 59.5%.

(2) To achieve high underflow concentration for ultrafine tailings, flocculant dosage should be minimized while keeping overflow turbidity within acceptable limits. And solid flux increased with feed concentration up to 8%, beyond which it decreased.

(3) At the same bed height, underflow concentration is lower during the bed descent phase compared to the continuous feeding phase, highlighting the influence of tailing residence time in DCT on thickening performance.

Author Contributions: Conceptualization, X.L., A.W. and J.W.; methodology, X.L. and J.W.; validation, X.L. and J.W.; formal analysis, J.W. and Z.D.; investigation, X.L. and Z.D.; data curation, X.L.; writing—original draft preparation, J.W. and Z.D.; writing—review and editing, X.L., A.W. and J.W.; supervision, X.L. and A.W.; project administration, X.L. and J.W.; funding acquisition, X.L., A.W. and J.W. All authors have read and agreed to the published version of the manuscript.

Funding: This research study was funded by the National Natural Science Foundation of China (no. 52074121, 52130404), the Postdoctoral Fellowship Program (Grade C) of China's Postdoctoral Science Foundation under grant number GZC20230237, a fellowship from the China Postdoctoral Science Foundation (no. 2023M730222), the Fundamental Research Funds for the Central Universities, and the Youth Teacher International Exchange and Growth Program (no. QNXM20230012).

Data Availability Statement: Data are available on request due to restrictions.

Conflicts of Interest: The authors declare that they have no known competing financial interest or personal relationships that could have appeared to influence the work reported in this paper.

References

1. Li, P.; Cai, M. Challenges and New Insights for Exploitation of Deep Underground Metal Mineral Resources. *Trans. Nonferrous Met. Soc. China* **2021**, *31*, 3478–3505. [CrossRef]
2. Ju, J.; Han, J.; Feng, C. Evaluation and Development Path of Comprehensive Utilization of Mineral Resources in China. *China Min. Mag.* **2024**, *33*, 14–25.
3. Walske, M.; McWilliam, H.; Doherty, J.; Fourie, A. Influence of Curing Temperature and Stress Conditions on Mechanical Properties of Cementing Paste Backfill. *Can. Geotech. J.* **2016**, *53*, 148–161. [CrossRef]
4. Al-moselly, Z.; Fall, M. Sulphate Influence on Strength Development of Cemented Paste Backfill with Superplasticizer under Field-like Curing Conditions. *Constr. Build. Mater.* **2024**, *451*, 138788. [CrossRef]
5. Sari, M.; Yilmaz, E.; Kasap, T. Long-Term Ageing Characteristics of Cemented Paste Backfill: Usability of Sand as a Partial Substitute of Hazardous Tailings. *J. Clean. Prod.* **2023**, *401*, 136723. [CrossRef]
6. Wang, J.; Wu, A.; Wang, M.; Ruan, Z. Experimental Investigation on Flow Behavior of Paste Slurry Transported by Gravity in Vertical Pipes. *Processes* **2022**, *10*, 1696. [CrossRef]
7. Wu, A.; Ruan, Z.; Li, C.; Wang, S.; Wang, Y.; Wang, J. Numerical Study of Flocculation Settling and Thickening of Whole-Tailings in Deep Cone Thickener Using CFD Approach. *J. Cent. South Univ.* **2019**, *26*, 711–718. [CrossRef]
8. Ruan, Z.; Wu, A.; Jiao, H.; Li, C.; Li, G.; Mo, Y.; Wang, H. Advances and Trends on Thickening of Full-Tailings Slurry in China. *Chin. J. Nonferrous Met.* **2022**, *32*, 286–301. [CrossRef]
9. Zhang, L. Production of Bricks from Waste Materials—A Review. *Constr. Build. Mater.* **2013**, *47*, 643–655. [CrossRef]
10. Ahmari, S.; Zhang, L. Production of Eco-Friendly Bricks from Copper Mine Tailings through Geopolymerization. *Constr. Build. Mater.* **2012**, *29*, 323–331. [CrossRef]
11. Lemanowicz, M.; Jach, Z.; Kilian, E.; Gierczycki, A. Ultra-Fine Coal Flocculation Using Dual-Polymer Systems of Ultrasonically Conditioned and Unmodified Flocculant. *Chem. Eng. J.* **2011**, *168*, 159–169. [CrossRef]
12. Wickramasinghe, S.R.; Leong, Y.K.; Mondal, S.; Liow, J.L. Influence of Cationic Flocculant Properties on the Flocculation of Yeast Suspensions. *Adv. Powder Technol.* **2010**, *21*, 374–379. [CrossRef]
13. Li, C.; Chen, G.; Ruan, Z.; Hou, H. Dynamic Evolution Law of Floc Structure in Whole Process of Tailings Thickening. *Chin. J. Nonferrous Met.* **2023**, *33*, 1318–1332. [CrossRef]
14. Zheng, D.; Song, W.; Tan, Y.; Cao, S.; Yang, Z.; Sun, L. Fractal and Microscopic Quantitative Characterization of Unclassified Tailings Flocs. *Int. J. Miner. Metall. Mater.* **2021**, *28*, 1429–1439. [CrossRef]
15. Wang, D.; Wang, D.; Wang, K.; Yeung, A.; Liu, Q. Enhancing the Dewatering of Oil Sands Mature Fine Tailings by Coagulation-Flocculation and Pressure Filtration with Tannic Acid-Mediated Polymeric Complex Network. *Sep. Purif. Technol.* **2024**, *335*, 126194. [CrossRef]
16. Motta, F.L.; Gaikwad, R.; Botha, L.; Soares, J.B.P. Quantifying the Effect of Polyacrylamide Dosage, Na^+ and Ca^{2+} Concentrations, and Clay Particle Size on the Flocculation of Mature Fine Tailings with Robust Statistical Methods. *Chemosphere* **2018**, *208*, 263–272. [CrossRef]
17. Wang, H.; Yang, Y.; Guo, J. Thickening Dehydration Performance and Flocculation Mechanism of Ultrafine Tailings Based on Dual Flocculation. *J. Cent. South Univ. Sci. Technol.* **2023**, *54*, 3597–3608. [CrossRef]
18. Thompson, D.K.; Motta, F.L.; Soares, J.B.P. Investigation on the Fl Occulation of Oil Sands Mature Fi Ne Tailings with Alkoxysilanes. *Miner. Eng.* **2017**, *111*, 90–99. [CrossRef]
19. Ruan, Z.; Wu, A.; Wang, Y.; Wang, Y.; Wang, J. Effect of Flocculation Sedimentation on the Yield Stress of Thickened Ultrafine Tailings Slurry. *Chin. J. Eng.* **2021**, *43*, 1276–1282.
20. Wu, A.; Ruan, Z.; Wang, J.; Yin, S.; Ai, C. Optimizing the Flocculation Behavior of Ultrafine Tailings by Ultra-Flocculation. *Chin. J. Eng.* **2019**, *41*, 981–986. [CrossRef]
21. Quezada, G.R.; Ramos, J.; Jeldres, R.I.; Robles, P.; Toledo, P.G. Analysis of the Flocculation Process of Fine Tailings Particles in Saltwater through a Population Balance Model. *Sep. Purif. Technol.* **2020**, *237*, 116319. [CrossRef]
22. Qi, C.; Ly, H.B.; Chen, Q.; Le, T.T.; Le, V.M.; Pham, B.T. Flocculation-Dewatering Prediction of Fine Mineral Tailings Using a Hybrid Machine Learning Approach. *Chemosphere* **2020**, *244*, 125450. [CrossRef] [PubMed]
23. Yang, Q.; Yang, S.; Zhang, R. Flocculation Sedimentation Test of Ultrafine Tailings Based on Turbidity of Supernatant Liquid. *Gold Sci. Technol.* **2022**, *30*, 948–957.
24. Govedarica, A.; Molina Bacca, E.J.; Trifkovic, M. Structural Investigation of Tailings Flocculation and Consolidation via Quantitative 3D Dual Fluorescence/Reflectance Confocal Microscopy. *J. Colloid Interface Sci.* **2020**, *571*, 194–204. [CrossRef]
25. Zou, Y.; Liu, Q.; Liu, W. Study on the Relation between Tailing Particle Size and Tailing Slurry Underflow Concentration. *Adv. Civ. Eng.* **2022**, 5449032. [CrossRef]
26. Wang, X.; Zhao, J.; Zhang, D. Optimal Prediction Model of Flocculating Sedimentation Velocity of Unclassified Tailings. *Chin. J. Nonferrous Met.* **2015**, *25*, 793–798. [CrossRef]
27. Zhang, Q.; Wang, S.; Wang, X. Influence Rules of Unit Consumptions of Flocculants on Interface Sedimentation Velocity of Unclassified Tailings Slurry. *Chin. J. Nonferrous Met.* **2017**, *27*, 318–324. [CrossRef]

28. Xiao, C. *Research on Intelligent Prediction Model Based on Depth Thickening Deductive Mechanism of Unclassed Tailings*; Central South University: Changsha, China, 2022.
29. Wang, S.; Wei, M.; Tao, T.; Song, X.; Liu, W.; Yu, H. Internal Structure Evolution Characteristics of High Concentration Unclassified Tailings Mortar Containing APAM. *Chin. J. Nonferrous Met.* **2022**, *32*, 3553–3566. [CrossRef]

Disclaimer/Publisher's Note: The statements, opinions and data contained in all publications are solely those of the individual author(s) and contributor(s) and not of MDPI and/or the editor(s). MDPI and/or the editor(s) disclaim responsibility for any injury to people or property resulting from any ideas, methods, instructions or products referred to in the content.